

Stress-Induced Martensitic Transformation in Metastable Austenitic Stainless Steels: Effect on Fatigue Crack Growth Rate

Z. Khan and M. Ahmed

This paper addresses the influence of cyclic stress-induced martensitic transformation on fatigue crack growth rates in metastable austenitic stainless steels. At low applied stress and mean stress values in AISI type 301 stainless steel, fatigue crack growth rate is substantially retarded due to a cyclic stress-induced γ-α' and γ-ε martensitic transformation occurring at the crack-tip plastic zone. It is suggested that the transformation products produce a compressive residual stress at the tip of the fatigue crack, which essentially lowers the effective stress intensity and hence retards the fatigue crack growth rate. At high applied stress or mean stress values, fatigue crack growth rates in AISI type 301 steels become almost equal to those of stable AISI type 302 alloy. As the amount of transformed products increases (with an increase in applied or mean stress), the strain-hardening effect brought about by the transformed martensite phase appears to accelerate fatigue crack growth, offsetting the contribution from the compressive residual stress produced by the positive volume change of $\gamma \rightarrow \alpha'$ or ε transformation.

Keywords
austenitic stainless steels, crack growth rate, fatigue, stress-induced transformation

1. Introduction

METASTABLE austenitic stainless steels are known to undergo a martensitic phase transformation when subjected to plastic deformation (Ref 1-7). Since fatigue is considered to involve a plastic (microplastic) deformation process, metastable austenitic stainless steels are also known to undergo a martensitic phase transformation during cyclic loading (Ref 8-12). This phase transformation is suggested to be localized mainly at the crack-tip region and thus to influence the crack propagation characteristics of the alloy.

Two different martensitic phases, α'-martensite (body-centered cubic) and ε-martensite (hexagonal close-packed) are known to form (Ref 5, 7, 9). Pineau and Pelloux (Ref 13) investigated the influence of strain-induced martensitic transformation on fatigue crack growth rate in Fe-Cr-Ni metastable austenitic stainless steels and reported that such rates in these alloys are strongly temperature dependent in the M_s-M_d temperature range. At a given ΔK level, the crack growth rates have been shown to decrease with decreasing temperature, while the fraction of strain-induced $\gamma \rightarrow \alpha'$ phase transformation at the tip of the fatigue crack increased. Comparing the fatigue crack growth rates in martensitic and austenitic steels, Bathias and Pelloux (Ref 14) have indicated that rates in metastable stainless steels are an order of magnitude lower than for maraging steels for $\Delta K < 32$ MPa$\sqrt{m}$ (30 ksi$\sqrt{in.}$). The excellent fatigue crack growth resistance of these steels has been related to the deformation-induced phase transformation taking place within the plastic zone and to the lower stacking fault energy of the alloys. The role of the phase transformation was assumed to provide extensive accommodating strain in the grain in front of the crack during crack arrest.

In related work in TRIP (transformation-induced plasticity) steels, Chanani et al. (Ref 15) also reported a beneficial effect of strain-induced martensitic transformation on fatigue growth rates. These steels were shown to exhibit lower fatigue crack growth rates than a number of alloy steels of similar strength levels, and they compared favorably with maraging steels in the low ΔK range. In this range, the experimental results were found to be in good agreement with the theoretical model, which predicted a relation of the form:

$$\frac{da}{dN} = C(\Delta K)^m$$

where ΔK is the crack-tip stress-intensity factor range, and C and m are material constants. The improvement in the fatigue crack growth rates in these alloys was attributed to the large, beneficial energy-absorbing effects of the strain-induced phase transformations that are usually observed in tensile and fracture toughness testing. Although the transformation is associated with rapid strain hardening, which is considered by some investigators to cause accelerated crack growth (Ref 16, 17), the beneficial effect is considered to offset the negative effects of rapid strain hardening and a decrease in the amount of strain to fracture due to the formation of martensite in a ductile austenite material.

A comparative study of AISI 201 and 202 indicated a shorter fatigue life for alloy 201, which transformed almost completely (~90%) to martensite. Alloy 202 transformed to a much smaller extent and exhibited a better fatigue resistance, indicating that the beneficial effect of the transformation is observed only in a certain range of the amount of transformed martensite (Ref 18). A related study on AISI 301 and 304 alloys again indicated that the beneficial effects of strain-induced transformation are observed only at small plastic strain amplitudes. Hertzberg (Ref 10) has shown that at strain amplitudes greater than 0.4%, the

Z. Khan and **M. Ahmed,** Mechanical Engineering Department, King Fahd University of Petroleum & Minerals, Dhahran 31261, Saudi Arabia.

formation of α′-martensite was detrimental to fatigue life. He has demonstrated that the improved fatigue resistance can be attributed to localized transformation at the crack tip, where it helps to relieve the stress concentration and creates favorable residual stresses in the plastic zone. This latter effect is due to the compressive stresses at the tip of the crack, which result from the positive volume change accompanying the $\gamma \rightarrow \alpha'$-martensite transformation.

Recent metallographic measurements of the size of transformed zone at the tip of a fatigue crack in an austenitic Fe-Ni-Al alloy have also been interpreted in terms of the volume change resulting from phase transformation (Ref 19). The compressive stresses resulting from γ-α' transformation are induced principally when the volume change is localized, retarding crack growth rate as a result of reduction in stress intensity at the crack tip (Ref 20).

In the present work, the influence of martensitic phase transformation on fatigue crack growth rates has been investigated in two austenitic stainless steels: AISI 301 and 302. The 301 alloy used is metastable and undergoes deformation-induced $\gamma \rightarrow \alpha'$-martensite phase transformation, whereas the 302 alloy remains essentially unchanged under the test conditions used. Metallographic, microhardness, and magnetic measurements were carried out to investigate the amount and distribution of martensite phase and its effect on fatigue crack growth rates.

2. Experimental Procedure

2.1 *Material and Specimen Preparation*

The commercial grades of the AISI 301 and 302 alloys used in this study had the chemical compositions and mechanical properties given in Tables 1 and 2. Single-edge notched specimens were machined from 1.5 mm thick sheet stock. Specimens (25 by 200 mm) were machined out such that the length was parallel to the rolling direction. A 9.5 mm deep saw cut was made in one edge with a diamond blade saw. The specimen geometry is shown in Fig. 1. After machining, specimens were sealed in evacuated Vycor capsules (Corning Glass Work, NY) and austenitized at 1050 °C for 30 min, followed by water quenching. After electropolishing, the specimens were heated in air for 30 min to aid the removal of any hydrogen that may have been picked up from the electrolyte during electropolishing.

Table 1 Chemical compositions of alloys

Element	Composition, wt% AISI 301	Composition, wt% AISI 302
Chromium	17.09	17.36
Nickel	7.25	10.21
Carbon	0.052	0.084
Silicon	0.48	0.64
Manganese	1.28	0.92
Sulfur	0.009	0.012
Nitrogen	0.038	0.046
Molybdenum	0.24	0.16

Table 2 Monotonic tensile properties

Property	AISI 301	AISI 302
Annealing temperature, °C	1050	1050
0.2% offset yield stress, MPa (ksi)	269 (39)	241 (35)
Ultimate tensile stress (UTS), MPa (ksi)	717 (104)	572 (83)
Elongation, %	71	58
Reduction in area, %	55	50.6
Hardness, VPH_{25g}	185	180
True fracture strength, MPa (ksi)	2185 (317)	827 (120)

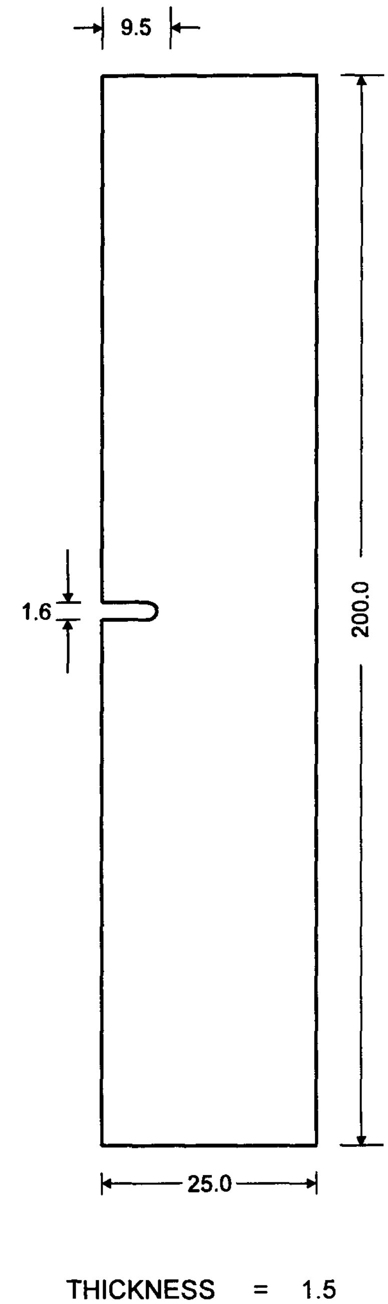

Fig. 1 Fatigue test specimen geometry. Dimensions given in millimeters.

2.2 *Mechanical Testing*

An electrohydraulic servocontrolled materials test system was used for fatigue testing. All fatigue tests were carried out using triangular waveform loading under load control. Relevant information on loading and other test conditions is included on the data plots. The crack length was measured to a precision of 0.1 mm using a traveling microscope mounted on a specially designed micrometer fixture. Crack growth was measured as the incremental growth during a given number of cycles. The stress-intensity factor range, ΔK, was obtained using:

$$\Delta K = Y \Delta \sigma \sqrt{\pi a} \qquad \text{(Eq 1)}$$

where Y is a function of a/w (w, width of specimen) and is obtained by:

$$Y = 1.99 - 0.41\left(\frac{a}{w}\right) + 18.70\left(\frac{a}{w}\right)^2 - 38.48\left(\frac{a}{w}\right)^3 + 53.85\left(\frac{a}{w}\right)^4 \qquad \text{(Eq 2)}$$

Fatigue tests were initially run at higher frequencies until the initiation of the fatigue crack. After initiation, tests were run at a frequency of 5 Hz.

2.3 *Magnetic Measurements*

Since the deformation-induced phase martensite is ferromagnetic and the rest of the phases present are paramagnetic, the amount of the transformed martensite is readily measurable through magnetic permeability or magnetic saturation measurements. The amount of α'-martensite formed from austenite during the test was determined by using a commercial ferrite detector. The detector, sensitive to magnetic permeability change, was calibrated directly in volume percent magnetic phase with an accuracy of ±0.5%.

2.4 *Metallography*

Both halves of the fatigue-fractured specimens were retained for metallographic and fractographic examinations. Specimens for optical metallographic examination were obtained by carefully cutting small sections from the fractured halves using a slow-speed diamond cutoff wheel. The electropolishing was carried out in the same way as described for specimen preparation. One set of specimens was etched by swabbing for 2 to 5 min with a freshly prepared solution of 10 mL nitric acid, 10 mL glacial acetic acid, 15 mL hydrochloric acid, and a few drops of glycerine. Some electropolished specimens were also etched using the α' stain etch technique, described elsewhere (Ref 21), to obtain better metallographic observation of the transformation products. Exposure of the specimen to a boiling saturated solution of chromic acid and sodium hydroxide for 3 to 4 h produced excellent delineation of the α' phase. To make sure that some of the parallel-sided bands that appeared in the acid-etched structure were not slip lines, one specimen of type 302 alloy was also given a stain etch treatment. The α' stain etch solution was found to have no effect on the slip lines, and it was thus assumed that all the darkened areas in the structure were in fact the transformed α' phase.

2.5 *Microhardness Measurements*

Microhardness measurements were used to determine the plastic zone size at the fatigue crack. These measurements were made after fracture at different positions along the crack in a direction perpendicular to the fracture surface. A diamond pyramid indentor was used with a load of 25 g.

3. Results and Discussion

3.1 *Monotonic Tensile Tests*

The results of tensile testing are reported in Fig. 2, which shows tensile stress versus strain and volume percent magnetic phase versus strain curves for alloys 301 and 302. The mono-

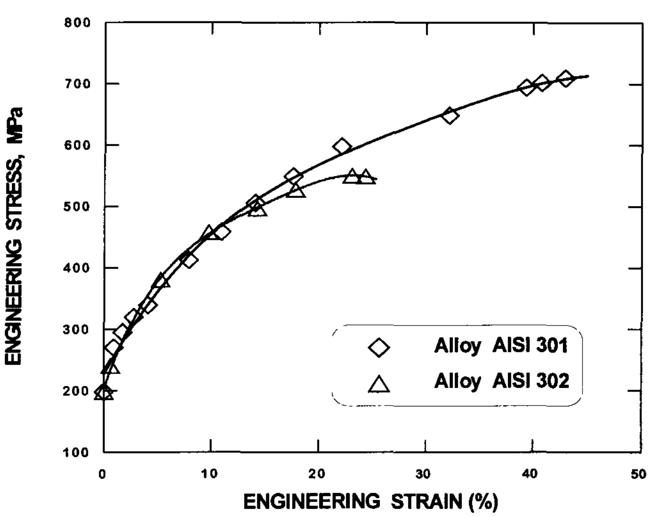

(a)

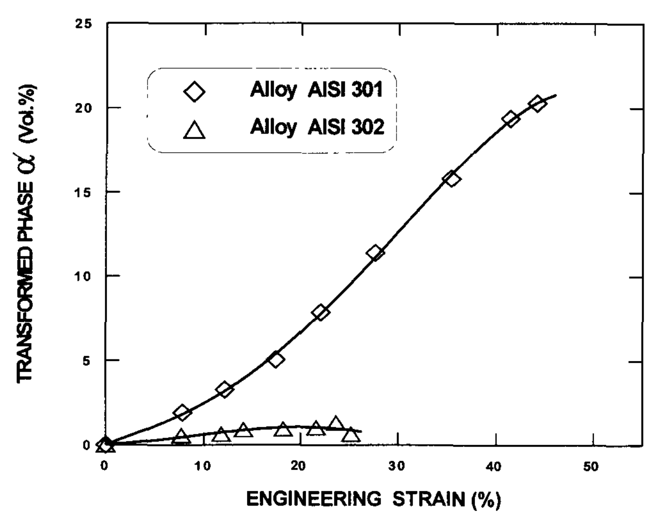

(b)

Fig. 2 Tensile stress versus strain (a) and magnetic volume percent versus strain (b) for AISI 301 and 302 alloys tonic tensile properties are listed in Table 2. As the results indicate, despite having almost similar chemical compositions, alloy 301 exhibits a higher UTS and a higher amount of ductility than alloy 302. Figure 2 also shows that a substantial amount of deformation-induced transformation is produced in alloy 301 during the ferrite deformation, whereas the alloy 302 microstructure remains unchanged. This indicates that the formation of martensite increases both the strength and the ductility of austenitic stainless steels undergoing martensitic formation. This observation is confirmed by many investigators (Ref 22-25).

3.2 *Fatigue Crack Propagation*

A comparison of fatigue crack growth rates in type 301 and type 302 stainless steels has been made in Fig. 3 to 5. As shown in Fig. 3, the crack growth rate in 301 alloy is lower than that for alloy 302 by a factor of four for all values of ΔK.

A survey of Fig. 3 to 5 reveals an interesting point regarding the effect of mean stress on the relative difference in the crack growth rates between the two alloys. Increasing the mean stress for the same value of R ($R = 0.05$) results in a decrease in the magnitude of the difference in crack growth rate between the two alloys. At the value of mean stress ($\sigma_{mean} = 90.5$ MPa), there is only a very small difference between the crack growth rates of the two alloys (see Fig. 5).

A comparison of the fatigue crack propagation lives of the two alloys shows a significant improvement in fatigue life for alloy 301 at lower values of applied stress (see Fig. 6). At higher stress levels, the difference in the lives of the two alloys becomes less and less pronounced. These observations, together with the observations regarding the effect of increasing mean stress on fatigue crack growth rates, suggest that the beneficial effect of the martensitic phase transformation in retarding crack growth rates and enhancing fatigue life in alloys capable of undergoing stress-induced transformation may occur only under low applied and mean stress levels. It may be true that the beneficial effect is produced only when small amounts of martensite, corresponding to lower values of mean and cyclic load levels, have formed at the crack tip. Incidentally, a comparative study of AISI 201 and 202 stainless steels has reported a shorter life for alloys that transform almost completely (~90%) to α′-martensite, as compared to those that transform to a much smaller extent (Ref 18).

The beneficial effect produced by the formation of α′-martensite at the tip of the fatigue crack due to stress-induced transformation of γ phase in alloy 301 could be explained in the following way. Fatigue crack propagation takes place as a result of damage at the crack tip caused by repeated stressing. If we consider a tiny element of volume ahead of the crack tip, it will experience increasing magnitude of strain amplitudes as

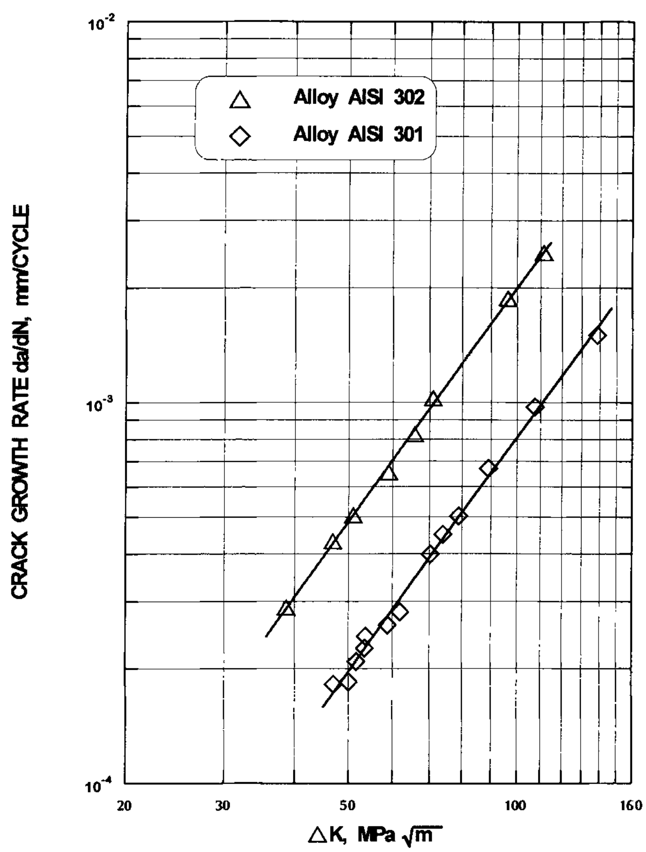

Fig. 3 Comparison of fatigue crack growth rates for AISI 301 and 302 alloys cycled to fracture at $R = 0.05$ and $\sigma_{mean} = 66$ MPa

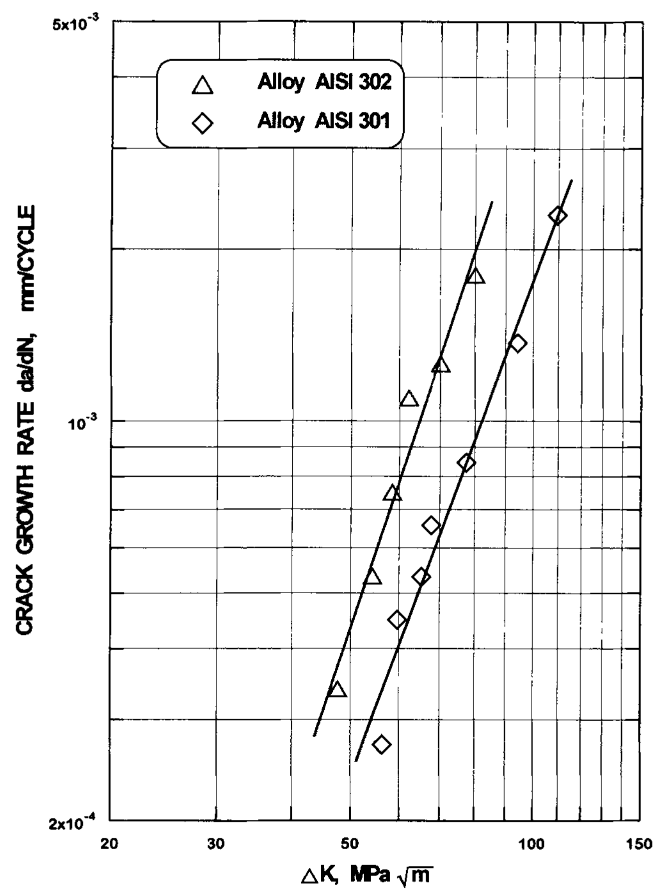

Fig. 4 Comparison of fatigue crack growth rates for AISI 301 and 302 alloys cycled to fracture at $R = 0.05$ and $\sigma_{mean} = 77.9$ MPa

the crack propagates toward it (due to increasing ΔK). The high cyclic strains cause $\gamma \rightarrow \alpha'$-martensite transformation at the tip of the fatigue crack. This transformation is associated with two important effects. First, martensite formation tends to increase the effective strain-hardening rate (Ref 17). This strain hardening is said to enable the crack to grow without gross deformation; that is, it reduces the amount of plastic strains required to cause fracture (Ref 16). This means that the rapid increase in strain-hardening rate due to the formation of martensite at the tip of the fatigue crack will result in an acceleration of the crack growth rate. On the other hand, the formation of α'-martensite is also associated with an increase in the specific volume. This volume increase induces a compressive stress in the transformed zone lying at the tip of the fatigue crack (Ref 9, 18-20). This compressive stress reduces the stress amplitude at the crack tip, thus lowering the crack-tip stress intensity. Consequently, this will decrease the fatigue crack growth rate.

It is evident now that deformation-induced martensitic transformation at the tip of the fatigue crack may produce two opposing influences on the crack propagation rate. The beneficial effect is obtained when the crack growth accelerating effect caused by the strain hardening due to the formation of α'-martensite is largely offset by the deceleration effect produced by the positive volume change occurring at the crack tip as a result of the transformation. It is reasonable to believe, therefore, that at low mean stress values the deceleration effect produced by the volume change associated with the formation of α'-martensite in alloy 301 may be largely offsetting the crack growth accelerating effect produced by strain hardening. At higher mean stress, however, the accelerating effect due to rapid strain hardening rate as a result of formation of large amounts of α'-martensite may be overshadowing the decelerating effect of volume change.

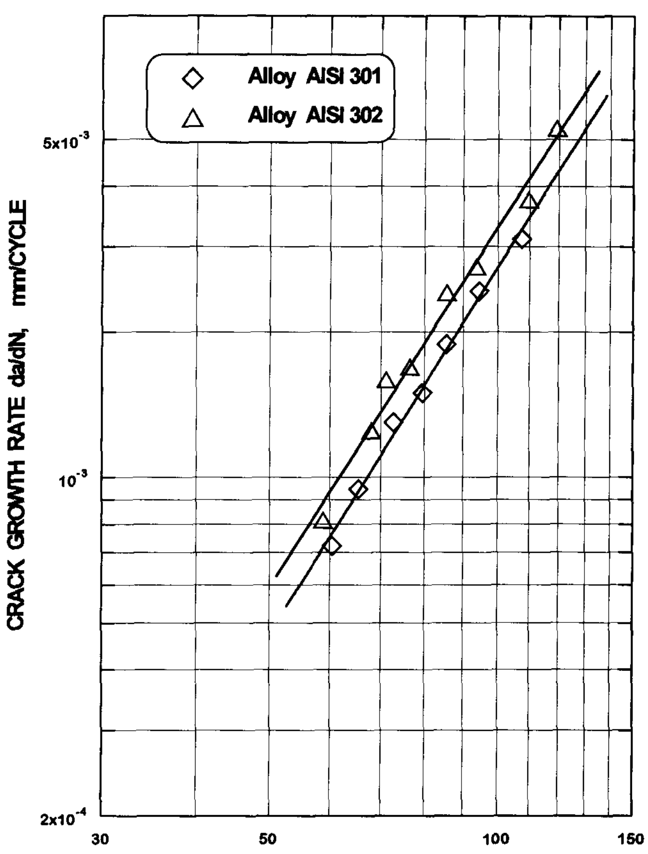

Fig. 5 Comparison of fatigue crack growth rates for AISI 301 and 302 alloys cycled to fracture at $R = 0.05$ and $\sigma_{mean} = 90.5$ MPa

3.3 *Plastic Zone*

The results of plastic zone size measurements by microhardness testing are reported in Fig. 7. The hardness indentations were made along directions perpendicular to the fracture surface at different crack lengths so as to cover a range of ΔK values. Figure 7 shows two typical plots of hardness versus distance from the fractured surface for types 301 and 302 stainless steel. The alloy 301 hardness curve presents two sharp drops in hardness, corresponding to the presence of two zones

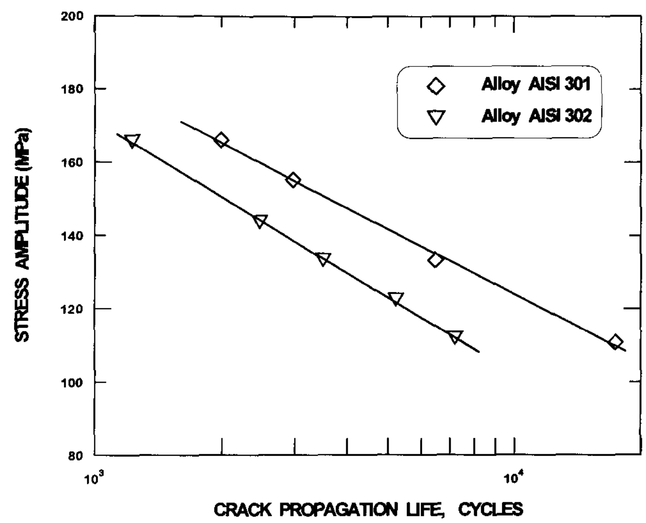

Fig. 6 Stress amplitude versus fatigue crack propagation life for AISI 301 and 302 alloys cycled at $R = 0.05$

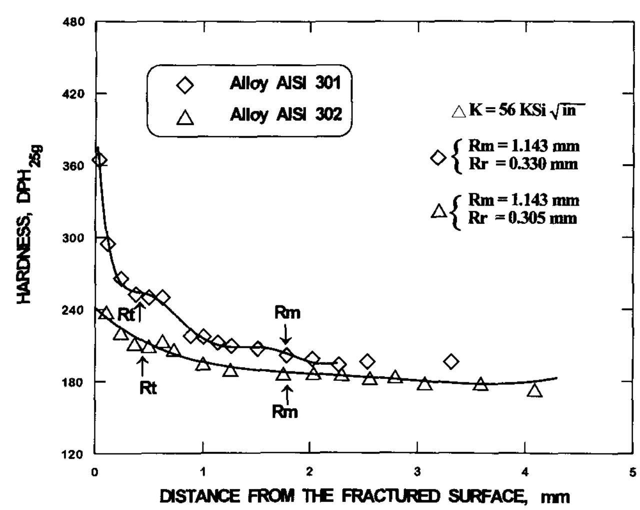

Fig. 7 Comparison of hardness versus distance from the fractured surface curves for AISI 301 and 302 alloys

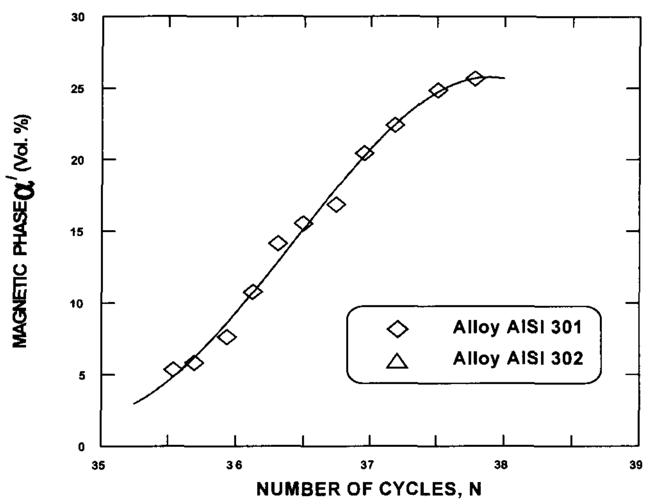

(a)

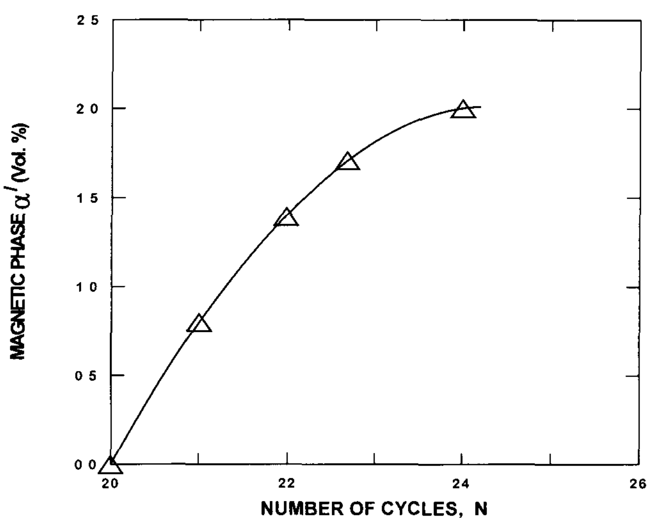

(b)

Fig. 8 Change in volume percent of magnetic phase during fatigue of AISI 301 and 302 alloys

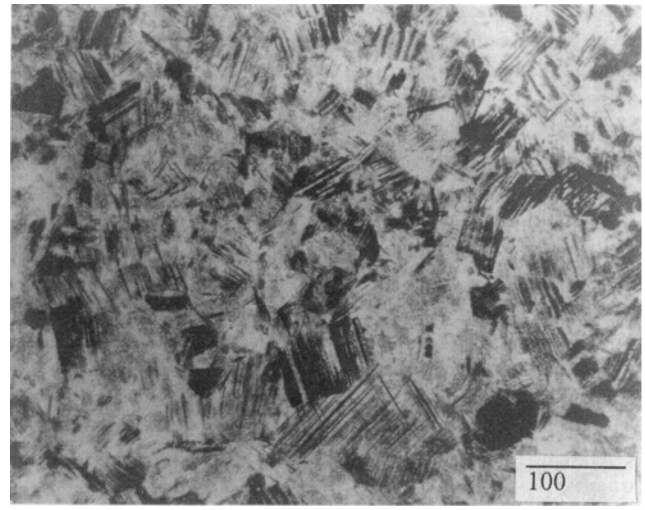

Fig. 9 Optical micrograph (stain etch) showing the transformation products 2 mm ahead of the crack tip. Transformed phase, 16.5 vol%

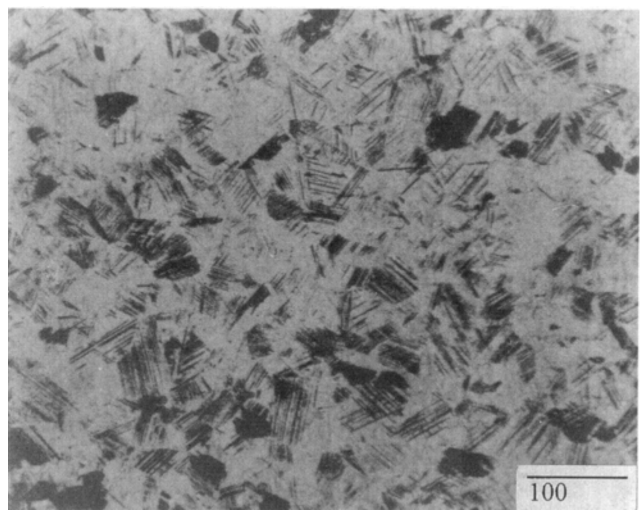

Fig. 10 Optical micrograph (stain etch) showing the transformation products 3 mm ahead of the crack tip. Transformed phase, 8.5 vol%

of plasticity. These two zones represent the cyclic and monotonic plastic zones at the tip of the crack. Similar results were reported by Rice (Ref 26).

Figure 8 shows the results of magnetic phase measurement for the alloy 301 specimen during fatigue testing. It can be seen that the magnetic phase continually increased with the number of cycles until the final fracture (Fig. 8a). In alloy 302, only a negligible amount of magnetic phase was formed under similar testing conditions (Fig. 8b). The indication here is that type 301 is a metastable alloy that can undergo deformation-induced martensite phase transformation when stressed at room temperature, whereas type 302 is a stable alloy and experiences no appreciable change in microstructure when similarly stressed.

3.4 *Metallographic Study*

Optical metallographic results were in general agreement with the microhardness measurements in that the martensitic phase is localized to the transformation zone at the crack tip (Fig. 9). The amount of transformed phase in alloy 301 seems to fall fairly abruptly at a distance greater than about 1 mm from the crack tip (Fig. 10). This corresponded roughly with the drop in hardness after the plateau (Fig. 9). Traces of transformation products were seen out to 4 mm or more from the fracture surface. Two different morphologies of the transformed martensite were observed, as can be seen in Fig. 9. Figure 11 represents an area about 3 mm from the crack tip and shows distinctly that two different transformation products are produced. Areas labeled A represent blocky and feathery patches, whereas areas labeled B are more lathlike. In AISI 302, the transformation produced was distributed about the crack tip in much the same way as in AISI 301, but in much smaller amounts. Furthermore, in alloy 302 the transformation product was largely of the thin plate type.

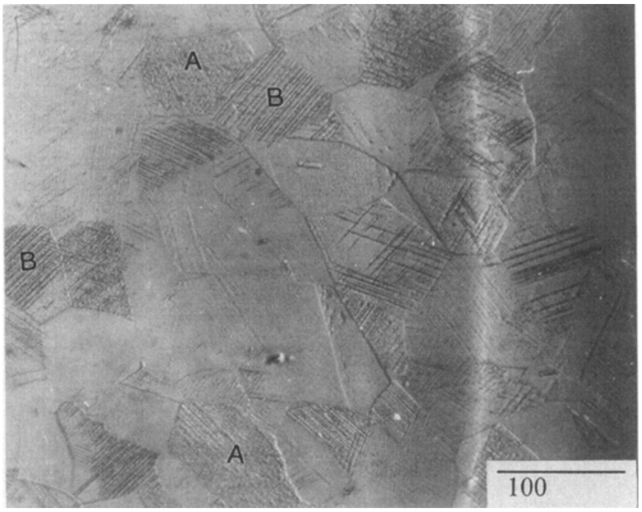

Fig. 11 Micrograph showing two different transformed phases. Areas labeled A represent α'-martensite; areas labeled B represent ε-martensite.

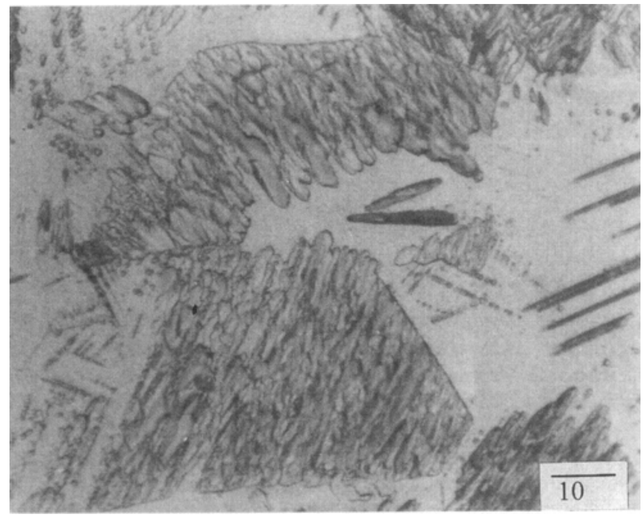

Fig. 12 Morphology of stress-induced transformation product α'-martensite

Interestingly, the transformation product found closer to the crack-tip region appeared to have a more blocky and patchy morphology and a more parallel-sided band morphology moving away from the crack tip. It is suggested that the parallel-sided bands are actually ε phase, which form initially under low stress and with a gradual increase in stress transform to either α' or $\gamma \rightarrow \alpha'$. Transformation in large amounts obscures the ε phase. Higher-magnification micrographs (Fig. 12 and 13) clearly show the different morphologies of the transformed phases.

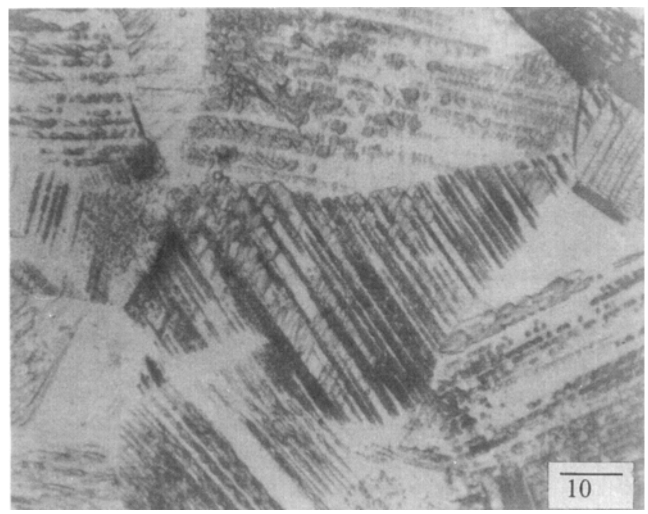

Fig. 13 Morphology of stress-induced transformation product ε-martensite

4. Conclusions

- Metastable austenitic stainless steel type AISI 301 exhibits significantly lower fatigue crack growth rates than the stable alloy type AISI 302 at low mean stress values.
- At high mean stress values, the fatigue crack growth rates in alloy 301 approach those of alloy 302.
- The lower fatigue crack growth rate in alloy 301 is attributed to the formation of deformation-induced martensite phase within the crack-tip plastic zone.
- The martensitic transformation results in a positive volume change at the crack tip. A compressive stress is produced at the crack tip, which lowers the stress amplitude and thus reduces the crack-tip stress intensity. Consequently, fatigue crack growth rate is retarded.
- At higher values of mean stress, the beneficial effect of martensitic transformation on fatigue crack growth rate is substantially offset by the accelerating effect on fatigue crack growth rate produced by the increase in the strain-hardening rate of the alloy due to large amounts of martensite formation.

References

1. T. Angel, *J. Iron Steel Inst.*, Vol 177, 1954, p 165
2. R. Lagnborg, *Acta Metall.*, Vol 12, July 1964
3. J.F. Breedis and L. Kaufman, *Metall. Trans.*, Vol 2, 1971, p 2359
4. F. Lecroisey and A. Pineau, *Metall. Trans.*, Vol 3, 1972, p 387
5. F. Abrassart, *Metall. Trans.*, Vol 4, 1973, p 2205
6. S.C. Tjong and N.J. Ho, *Mater. Sci. Eng. A*, Vol 102, 1988, p 125
7. S.G.S. Raman and K.A. Padmanabhan, *J. Mater. Sci. Lett.*, Vol 13, 1994, p 389
8. E. Hornbogen, *Acta Metall.*, Vol 26, 1978, p 147
9. D. Hennessy, G. Steckel, and C. Altstetter, *Metall. Trans.*, Vol 7A, 1976, p 415
10. R.W. Hertzberg, *Metall. Trans.*, Vol 5, 1974, p 306
11. C. Laird, in *Fatigue Crack Propagation*, STP 415, ASTM, 1967, p 131
12. D.W. Hoepner, in *Fatigue Crack Propagation*, STP 415, ASTM, 1967, p 486
13. A.G. Pineau and R.M Pelloux, *Metall. Trans.*, Vol 5, 1974, p 1103
14. C. Bathias and R.M. Pelloux, *Metall. Trans.*, Vol 4, 1973, p 1265

15. G.R. Chanani, S.D. Antolovich, and W.W. Gerberich, *Metall. Trans.*, Vol 3, 1972, p 2661
16. B. Cotterell, *J. Basic Eng. (Trans. ASME)*, Vol 87, 1965, p 230
17. W.F. Barclay, in *Advances in Technology of Stainless Steels and Related Alloys*, STP 369, ASTM, 1963, p 26
18. G. Franke and C.J. Altstetter, *Metall. Trans.*, Vol 7A, 1976, p 1719
19. I. Wittkamp and E. Hornbogen, *Prakt. Metallogr.*, Vol 14, 1977, p 237
20. E. Hornbogen, *Acta Metall.*, Vol 26, 1978, p 147
21. R.P. Reed, *Acta Metall.*, Vol 10, 1962, p 865
22. J. Singh, *J. Mater. Sci.*, Vol 20, 1985, p 3157
23. R.G. Luther and T.R. Williams, *Mater. Sci.*, Vol II, 1977, p 219
24. P.C. Maxwell, A. Goldberg, and J.C. Shyne, *Metall. Trans.*, Vol 5, 1974, p 1319
25. D. Bhandarkar, V.F. Zackay, and E.R. Parker, *Metall. Trans.*, Vol 3, 1972, p 2619
26. J.R. Rice, in *Fatigue Crack Propagation*, STP 415, ASTM, 1967, p 247